

Temperature induced in-gap states in the band structure and the insulator-metal transition in LaCoO_3

S.G. Ovchinnikov,^{1,2,3,*} Yu.S. Orlov,^{1,†} I.A. Nekrasov,^{4,‡} and Z.V. Pchelkina^{5,§}

¹*Institute of Physics, Siberian Branch Russian Academy of Sciences, Krasnoyarsk 660036, Russia*

²*Siberian Federal University, Krasnoyarsk 660041, Russia*

³*Siberian Aerospace University, Krasnoyarsk 660014, Russia*

⁴*Institute for Electrophysics, Russian Academy of Sciences-Ural Division, Yekaterinburg 620016, Russia*

⁵*Institute of Metal Physics, Russian Academy of Sciences-Ural Division, Yekaterinburg 620990, Russia*

For many years a spin-state transition at $T \approx 100\text{K}$ and insulator - metal transition (IMT) at $T_{\text{IMT}} \approx 600\text{K}$ in LaCoO_3 remains a mystery. Small low-spin - high-spin spin gap $\Delta_S = E(\text{HS}) - E(\text{LS}) \sim 100\text{K}$ results in the spin-state transition. The large charge gap $2E_a \approx 2300\text{K}$ (E_a is the activation energy) vs. Δ_S and T_{IMT} implies that LaCoO_3 is not a simple narrow-gap semiconductor. Here we explain both the spin-state and IMT on the same footing. We obtain strong temperature dependent band structure in LaCoO_3 by the LDA+GTB method that incorporates strong electron correlations, covalence and spin-orbital interaction exactly inside the CoO_6 cluster and the intercluster hopping between different multielectron configurations by perturbation theory for Hubbard X-operators.

PACS numbers: 72.80.Ga, 71.30.+h, 71.70.Ch, 75.30.Wx

The perovskite-oxide LaCoO_3 has been studied intensely for many years due its unique magnetic properties and related insulator-metal transition (IMT) [1, 2]. A gradual appearance of the paramagnetism above 50K from the nonmagnetic ground state is called the spin-state transition. Goodenough was the first who suggested that instead of the Hund's rule dictated high spin (HS) $S = 2$ the strong crystalline electric field results in the low spin (LS) $S = 0$ state for d^6 configuration of the Co^{3+} ion, and the energy difference is very small with the spin gap $\Delta_S = E(\text{HS}) - E(\text{LS}) \sim 100\text{K}$. The thermal population of the HS state provides the sharp increase of the magnetic susceptibility χ with a maximum around 100K . The nature of the excited spin state of Co^{3+} above the singlet $^1A_{1g}$ has been under debate (see for a recent review [3]). Besides the original $^5T_{2g}$ HS state with the $t_{2g}^4 e_g^2$ configurations [2] there were many indications on the intermediate spin (IS) $S = 1$ $^3T_{1g}$ state. The two stage model has been proposed with the LS-IS transition at 100K and IS-HS transition at $550 - 600\text{K}$ [4, 5]. Recent electronic spin resonance (ESR) [6], X-ray absorption spectroscopy (XAS) and X-ray magnetic circular dichroism (XMCD) [7] experiments prove that the lowest excited state is really the HS. Nevertheless the $^5T_{2g}$ term is splitted by the spin-orbital interaction in the low energy triplet with effective moment $\tilde{J} = 1$, and higher energy sublevels with $\tilde{J} = 2$ and $\tilde{J} = 3$ [8]. The large difference between the spin excitation gap Δ_S and the charge gap given by the activation energy for electrical conductivity $E_a \approx 0,1\text{eV}$ at low T indicates that LaCoO_3 is not a simple band insulator [9]. The second shallow maximum in χ near $500 - 600\text{K}$ is often related to the insulator-metal transition. Surprisingly for the IMT electrical conductivity σ does not seem to show any noticeable anomaly at this temperature [9]. Moreover the discrepancy between the large charge gap $2E_a \approx 2300\text{K}$ and the insulator-metal transition temperature $T_{\text{IMT}} \approx 600\text{K}$ implies that the IMT cannot be simply argued in terms of a narrow-gap semiconductor [10]. Here, we solved this problem by calculating the electronic band structure in the regime of strong electron correlations. We consider electron as the linear combination of quasiparticles (QP) given by excitations between the different multielectron configurations obtained by exact diagonalization of the CoO_6 cluster. With the Hubbard operators constructed within the exact cluster eigenstates we can calculate the QP band structure for the infinite lattice. The QP spectral weight is determined by the occupation numbers of the local multielectron configurations. We find that the thermal population of different sublevels of the $^5T_{2g}$ HS term splitted by the spin-orbital interaction results both in the spinstate transition and also in some new QP excitations. Of particular importance is the hole creation QP from the initial d^6 HS into the d^5 HS term, this QP appears to form the in-gap state inside the large charge-transfer gap $E_g \approx 1,5\text{eV}$. The intercluster hopping transforms this local QP into the in-gap band that lies just under the bottom of empty conductivity band and provides the insulating gap $2E_a \approx 0,2\text{eV}$ at $T = 100\text{K}$. It bandwidth increases with T , and overlaps with the conductivity band at $T = T_{\text{IMT}} = 587\text{K}$ resulting in the IMT. Hence our approach allows to treat both the low T spin-state transition and the high T IMT on the same footing.

LaCoO_3 as well as other strongly correlated oxides is a difficult problem for the ab initio band theory. The LDA calculations [11] incorrectly predict a metal for paramagnetic LaCoO_3 . Various methods have been applied to study effect of correlations on the LaCoO_3 electronic structure: LDA+U or GGA+U [12–15], dynamical mean-field theory [16]. Recent variational cluster approximation (VCA) calculation [17] based on the exact diagonalization of the

CoO₆ cluster gives a reasonably accurate description of the low temperature properties: the insulating nature of the material, the photoelectron spectra, the LS-HS spin-state transition. The main deficiency of the VCA is the failure to reproduce the high temperature anomalies in the magnetic and electronic properties associated with the IMT. The exact diagonalization of the multielectron Hamiltonian for a finite cluster provides a reliable general overview of the electronic structure of the correlated materials [18]. To incorporate the lattice effect several versions of the cluster perturbation theory are known [19, 20]. To calculate the band dispersion in the strongly correlated material one has to go beyond the local multielectron language. The natural tool to solve this problem is given by the Hubbard X-operators $X_f^{pq} = |p\rangle\langle q|$ constructed with the CoO₆ cluster eigenvectors $|p\rangle$ at site \vec{R}_f . All effects of the strong Coulomb interaction, spin-orbit coupling, covalence and the crystal field inside the CoO₆ cluster are included in the set of the local eigenstates E_p . Here p denotes the following quantum numbers: the number of electrons (both 3d Co and p of O), spin S and pseudoorbital moment \tilde{l} (or the total pseudomoment \tilde{J} due to spin-orbit coupling), the irreducible representation in the crystal field. A relevant number of electrons is determined from the electroneutrality, for stoichiometric LaCoO₃ $n = 6$. In the pure ionic model the corresponding energy level scheme for d^6 Co³⁺ has been obtained in [8]. Due to the covalence there is admixture of the ligand hole configurations $d^{n+1}\underline{L}$ and $d^{n+2}\underline{L}^2$ that is very well known in the X-ray spectroscopy [21]. Contrary to spectroscopy the electronic structure calculations require the electron addition and removal excitations. For LaCoO₃ it means the d^5 and d^7 configurations. The total low energy Hilbert space is shown in the fig. 1. Here the energy level notations are the same as in the ionic model [8] but all eigenstate contains the oxygen hole admixture due to the covalence effect. The calculation of the $n = 5, 6, 7$ eigenvectors for CoO₆ cluster with the spin-orbit coupling and the Coulomb interaction has been done in [22].

Following the generalized tight-binding (GTB) method [23] and its ab initio version LDA+GTB [24] we consider the electron annihilation operator at site f , orbital state λ (Co d or O p) and spin projection σ as the linear combination of the Hubbard operators

$$a_{f\lambda\sigma} = \sum_n \gamma_{\lambda\sigma}(n) X_f^n. \quad (1)$$

Here n numerates different pairs of indexes in $X_f^{pq} = |p\rangle\langle q|$ to describe the excitation from the initial state $|q\rangle$ to the final one $|p\rangle$. The matrix element $\gamma_{\lambda\sigma}(n)$ is calculated straightforwardly as the eigenvectors $\{|p\rangle\}$ are known from the exact diagonalization of CoO₆ cluster. In the X-operator representation the initial multielectron and multiorbital Hamiltonian has the same operator structure as the Hubbard model

$$H = \sum_{fp} E_p X_f^{pp} + \sum_{fgnm} t_{fg}^{mn} X_f^{m\dagger} X_g^n. \quad (2)$$

Here E_p is the local eigenstate. All intercluster Coulomb interactions and hopping are included in the \hat{t}_{fg} matrix and are treated perturbatively. The electron Green function

$$G_{\lambda\lambda'\sigma}(k, \omega) = \langle\langle a_{k\lambda\sigma} | a_{k\lambda'\sigma}^\dagger \rangle\rangle_\omega = \sum_{nm} \gamma_{\lambda\sigma}(n) \gamma_{\lambda'\sigma}(m) D^{mn}(k, \omega), \quad D_{fg}^{mn} = \left\langle\left\langle X_f^m \left| X_g^n \right. \right\rangle\right\rangle. \quad (3)$$

Its local part is found exactly

$$G_{\lambda\sigma}^{(0)}(k, \omega) = \sum_n |\gamma_{\lambda\sigma}(n)|^2 \frac{F(n)}{\omega - \Omega_n}. \quad (4)$$

Here $\Omega_n = E_p(N+1) - E_q(N)$ is the QP energy, $F(n) = \langle X_f^{pp} \rangle + \langle X_f^{qq} \rangle$ is the filling factor. This factor provides zero spectral weight for the excitations between two unoccupied states. The non-zero contribution to the Green function requires a participation of at least one occupied state in the QP $n = (p, q)$.

The electron removal spectrum determines the top of the valence band, the corresponding QP are shown in the fig. 1 by thin solid lines as the excitation from the $^1A_{1g}$ d^6 singlet in the $^2T_{2g}$ d^5 states with $\tilde{J} = 1/2$ and $\tilde{J} = 3/2$. There energies are

$$\Omega_{V1} = E(d^6, ^1A_1) - E(d^5, ^2T_2, \tilde{J} = 1/2), \quad \Omega_{V2} = E(d^6, ^1A_1) - E(d^5, ^2T_2, \tilde{J} = 3/2). \quad (5)$$

The bottom of empty conductivity band has the energy

$$\Omega_C = E(d^7, ^2E) - E(d^6, ^1A_1). \quad (6)$$

All these bands have nonzero QP spectral weight. The intercluster hopping results in the dispersion, $\Omega_n \rightarrow \Omega_n(k)$. In a simplest Hubbard-1 approximation for the \hat{t}_{fg} Green function is given by

$$\hat{D}^{-1}(k, \omega) = \hat{D}_0^{-1}(\omega) - \hat{t}(k), \quad (7)$$

the band structure is obtained from the dispersion equation

$$\det \|\delta mn(E - \Omega_n)/F(n) - t^{mn}(k)\| = 0. \quad (8)$$

In the LDA+GTB version the single-site electron energies as well as the interatomic hopping integrals of the p-d model has been obtained by Wannier function projection technique [25]. The LDA band structure of LaCoO₃ was obtained within linearized muffin-tin orbital (LMTO) basis set [26] using structural data for $T = 5K$ [27]. The calculated bands are in good agreement with the previous results [11]. The bands resulted from the projection procedure for five Co d-orbitals and three O p-orbitals completely reproduce the initial LDA bands. The local coordinate system with the axis directing towards oxygen atoms forming the octahedron around Co atom was used. The intra-atomic Hubbard and Hund parameters U and J have been calculated within the constrained LDA method [28]. The QP LDA+GTB band structure corresponds to the charge-transfer insulator [29] with the gap $E_g \approx 1.5eV$ (fig. 2) at $T = 0K$. This gap value is rather close to the VCA gap [17] and the experimental value $E_g \approx 1eV$ [10].

At finite temperature the thermal excitation over the spin-gap Δ_S into the $\tilde{J} = 1$ and over the gap $\Delta_S + 2\tilde{\lambda}$ into the $\tilde{J} = 2$ sublevels of the HS ${}^5T_{2g}$ state occurs. We take $\Delta_S = 140K$ and $\tilde{\lambda} = 185K$ following [6]. Partial occupation of the excited HS states results in the drastically change of the QP spectrum. For $T = 0K$ excitations from the 1A_1 d^6 singlet in the lowest 6A_1 d^5 term were forbidden due to spin conservation (the corresponding matrix element $\gamma_n = 0$, see (1)), and the excitation from $|d^6, \tilde{J} = 1\rangle$ in $|d^5, {}^6A_1\rangle$ has nonzero matrix element (shown by dashed line Ω_{V1}^* in the fig. 1) but zero filling factor as the excitation between two empty states. For $T \neq 0$ the filling factor for the Ω_{V1}^* and Ω_{V2}^* QP is non zero and is equal to the occupation number n_1 and n_2 of the states $|d^6, \tilde{J} = 1\rangle$ and $|d^6, \tilde{J} = 2\rangle$ correspondingly. The energies of these QP are

$$\Omega_{V1}^* = E(d^6, {}^5T_{2g}, \tilde{J} = 1) - E(d^5, {}^6A_1), \quad \Omega_{V2}^* = E(d^6, {}^5T_{2g}, \tilde{J} = 2) - E(d^5, {}^6A_1). \quad (9)$$

The energies of these QP appear to be slightly below the bottom of the conductivity band, see DOS at finite temperature in the fig. 2. Thus we have obtained that these temperature-induced QP states lies inside the charge-transfer gap, they are the in-gap states. Similar in-gap states are known to result from doping in the high temperature superconductors. The LaCoO₃ is unique because the in-gap states are induced by heating. The chemical potential lies in the narrow gap $2E_a \approx 0.2eV$ at $T = 100K$ between the in-gap states and conductivity band.

From the GTB dispersion equation (8) it is clear that the in-gap bandwidth is proportional to the occupation numbers n_1 and n_2 of the excited HS states. With further temperature increase the in-gap bands Ω_{V1}^* and Ω_{V2}^* become wider and finally overlap with the conductivity band Ω_C (fig. 2) at $T = T_{IMT} = 587K$. It should be clarified that the IMT in LaCoO₃ is not the thermodynamic phase transition, there is no any order parameter associated with the gap contrary to the classical IMT in VO₂, NiS etc.

Assuming that the carrier mobility is a smooth function of temperature we have estimated the temperature dependent conductivity as

$$\sigma(T) = \sigma_0 \exp(-E_a(T)/kT) \quad (10)$$

with the temperature dependent $E_a(T)$ given by the DOS calculations. The fitting parameter σ_0 was taken as $\sigma_0 = \sigma_{\text{exp}}(800K)$. The overall agreement of the calculated and experimental data from [9] is clear (see fig. 3). The deviations at the 300 – 350K we believe stem from some other interactions omitted in our calculations. There is similar anomaly in the thermal expansion coefficient in the same temperature range [30], so may be the spin-phonon and electron-phonon interactions are responsible for this discrepancy.

We have also calculated the average moment $\vec{J} = \vec{L} + \vec{S}$ as $J_{av} = \langle \hat{J}^2 \rangle^{1/2}$ as function of temperature (fig. 4). Here

$$\langle \hat{J}^2 \rangle = \sum_n \langle n | \hat{J}^2 | n \rangle \langle X^{nn} \rangle. \quad (11)$$

The expected for HS value $J_{av} \approx 2$ is reached only at $T \approx 1000K$. In the region of the spin-state transition at $T \approx 100K$ the value of J_{av} is close to 1. May be it is the reason why so many experimentalists have obtained the IS

$S = 1$ fitting their data by the state with definite spin. Temperature dependence of the magnetic susceptibility has the maximum at $T \approx 100K$ similar to many previous works with LS-HS scenario [9, 31].

Thus, we find that a correct definition of the electron in strongly correlated system directly results in the in-gap states during the spin-state transition due to the thermal population of the excited HS states. Close to the spin-state temperature region the in-gap states determine the value of the activation energy $E_a \approx 0.1eV$. Further temperature increase results in larger in-gap bandwidth and smaller E_a , and finally $E_a = 0$ at $T_{IMT} = 587K$. As concerns the weak maximum in the $\chi(T)$ close to the IMT it may be a small Pauli-type contribution from the itinerant carriers above T_{IMT} . We emphasize that instead of rather large difference in temperatures of the spin-state transition ($\sim 100K$) and the IMT ($600K$) the underlying mechanism is the same and is induced by the thermal population of the excited HS states.

Acknowledgements

We acknowledge discussions with G.A. Sawatzky, M.W. Haverkort, S.V. Nikolaev and V.A. Gavrichkov. This work is supported by the Siberian Branch of RAS and Ural Branch of RAS integration project 40, Presidium RAS Program 5.7, RFBR grant 09-02-00171-a, RFBR grant 10-02-00251 and Dynasty Foundation.

* Electronic address: sgo@iph.krasn.ru

† Electronic address: jso.krasn@mail.ru

‡ Electronic address: nekrasov@iep.uran.ru

§ Electronic address: pzv@ifmlrs.imp.uran.ru

- [1] G. H. Jonker, and J. H. Van Santen, Physica 19, 120 (1953).
- [2] P. M. Raccah, and J. B. Goodenough, Phys. Rev. 155, 932 (1967).
- [3] N. B. Ivanova et al., Physics: Uspehi Fizicheskikh Nauk 179 (8), 837 (2009).
- [4] R. H. Potze, G. A. Sawatzky, and M. Abbate, Phys. Rev. B 51, 11501 (1995).
- [5] T. Saitoh, T. Mizokawa, A. Fujimori, M. Abbate, Y. Takeda, and M. Takano, Phys. Rev. B 55, 4257 (1997).
- [6] S. Noguchi, S. Kawamata, K. Okuda, H. Najiri, and M. Motokawa, Phys. Rev. B 66, 094404 (2002).
- [7] M. W. Haverkort et al., Phys. Rev. Lett. 97, 176405 (2006).
- [8] Z. Ropka, and R. J. Radwanski, Phys. Rev. B 67, 172401 (2003).
- [9] S. Yamaguchi, Y. Okimoto, H. H. Taniguchi, and Y. Tokura, Phys. Rev. B 53, R2926 (1996).
- [10] S. Yamaguchi, Y. Okimoto, and Y. Tokura, Phys. Rev. B 54, R11022 (1996).
- [11] P. Ravindran, P. A. Korzhavyi, H. Fjellvag, and A. Kjekshus, Phys. Rev. B 60, 16423 (1999).
- [12] M. A. Korotin, S. Yu. Ezhov, I. V. Solovyev, and V. I. Anisimov, Phys. Rev. B 54, 5309 (1996).
- [13] K. Knizek, P. Novak, and Z. Jirak, Phys. Rev. B 71, 054420 (2005).
- [14] S. K. Randey et al., Phys. Rev. B 77, 045123 (2008).
- [15] H. Hsu, K. Umemoto, M. Cococcioni, and R. Wentzcovitch, Phys. Rev. B 79, 125124 (2009).
- [16] L. Craco, and E. Muller-Hartmann, Phys. Rev. B 77, 045130 (2008).
- [17] R. Eder, Phys. Rev. B 81, 035101 (2010).
- [18] E. Dagotto, Rev. Mod. Phys. 66, 763 (1994).
- [19] T. Maier, M. Jarrel, Th. Pruschke, and M. H. Hettler, Rev. Mod. Phys. 77, 1027 (2005).
- [20] D. Senechal, and A.-M. Tremblay, Phys. Rev. Lett. 92, 126401 (2004).
- [21] M. Abbate et al., Phys. Rev. B 47, 16124 (1993).
- [22] Yu. S. Orlov, and S. G. Ovchinnikov, JETP 109, 322 (2009).
- [23] S. G. Ovchinnikov, and I. S. Sandalov, Physica C 161, 607 (1989).
- [24] M. M. Korshunov et al., Phys. Rev. B 72, 165104 (2005).
- [25] V. I. Anisimov et al., Phys. Rev. B 71, 125119 (2005).
- [26] O. K. Andersen, and O. Jepsen, Phys. Rev. Lett. 53, 2571 (1984).
- [27] P. G. Radaelli, and S.-W. Cheong, Phys. Rev. B 66, 094408 (2002).
- [28] G. Gunnarsson, O. K. Andersen, O. Jepsen, and J. Zaanen, Phys. Rev. B 39, 1708 (1989).
- [29] J. Zaanen, G. A. Sawatzky, and J. W. Allen, Phys. Rev. Lett. 55, 418 (1985).
- [30] K. Asai, O. Yokokura, and N. Nishimori, Phys. Rev. B 50, 3025-3032 (1994).
- [31] M. J. R. Hoch et al., Phys. Rev. B 79, 214421 (2009).

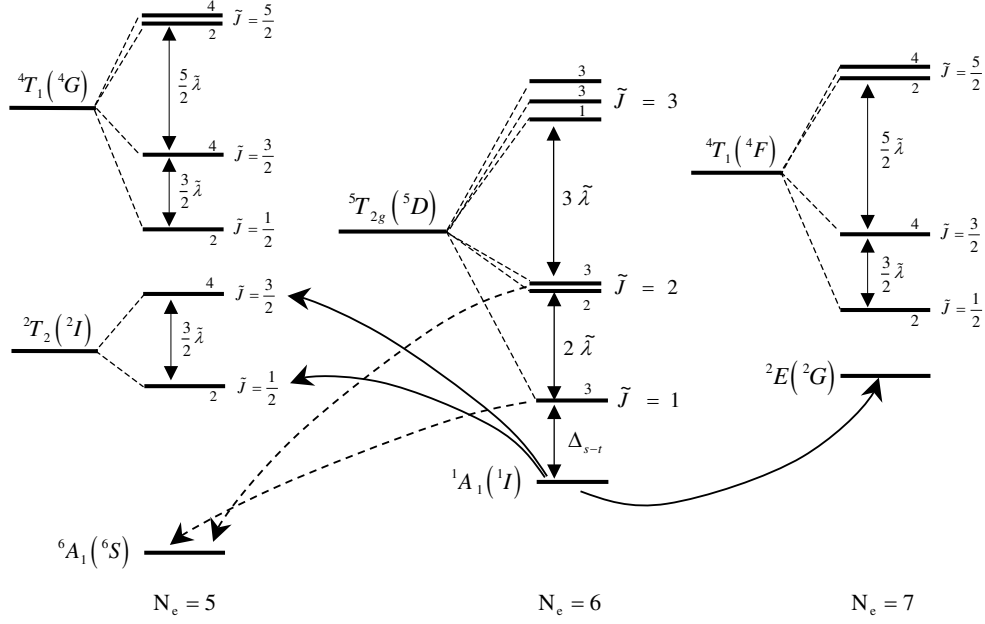


FIG. 1: The low energy part of the CoO₆ cluster Hilbert state for the electron numbers $N_e = 5, 6, 7$. Terms with given N_e are the mixtures of d^{N_e} , $d^{N_e+1}\underline{L}$ and $d^{N_e+2}\underline{L}^2$ configurations. At $T = 0$ only the $N_e = 6$ low spin term 1A_1 is occupied, the Fermi-type excitations from this term that form the top of the valence band ($d^6 \rightarrow d^5$) and the bottom of the conductivity band ($d^6 \rightarrow d^7$) are shown by the solid lines with arrow. The dashed lines denote the in-gap excitations with the spectral weight increasing with temperature due to the population the HS excited d^6 terms.

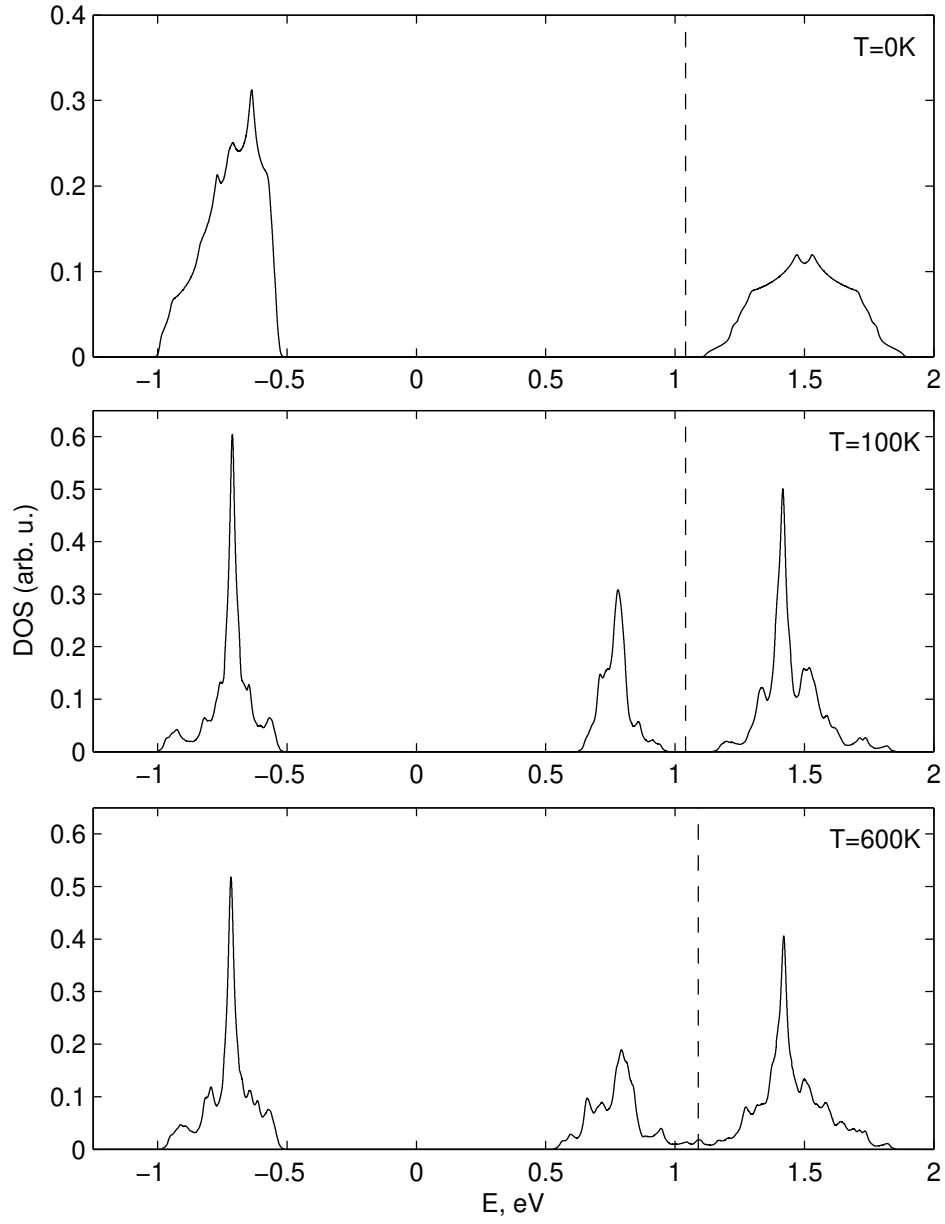


FIG. 2: Single particle density of states at different temperatures. At $T = 0K$ LaCoO_3 is the charge transfer insulator with the gap $E_g \approx 1.5eV$. At finite temperatures the in-gap band appears below the conductivity band with the temperature dependent activation energy. At $T = 100K$ $E_a \approx 0.1eV$. At $T = T_{IMT} = 587K$ $E_a = 0eV$, and above T_{IMT} the band structure is of the metal type.

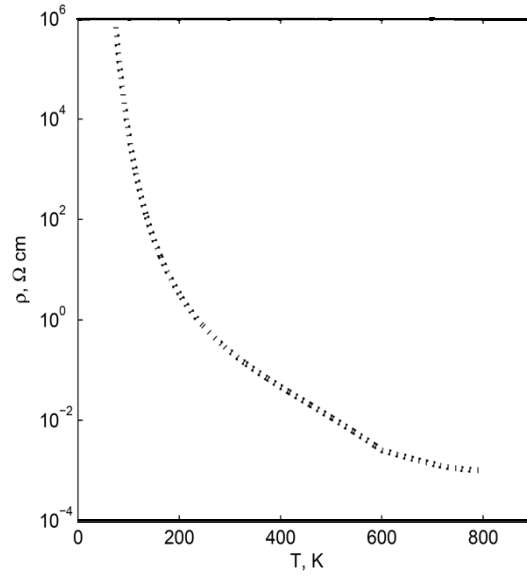


FIG. 3: The temperature dependence of the resistivity, solid line shows the experimental data [9] and dashed line is calculated from Eq.(4).

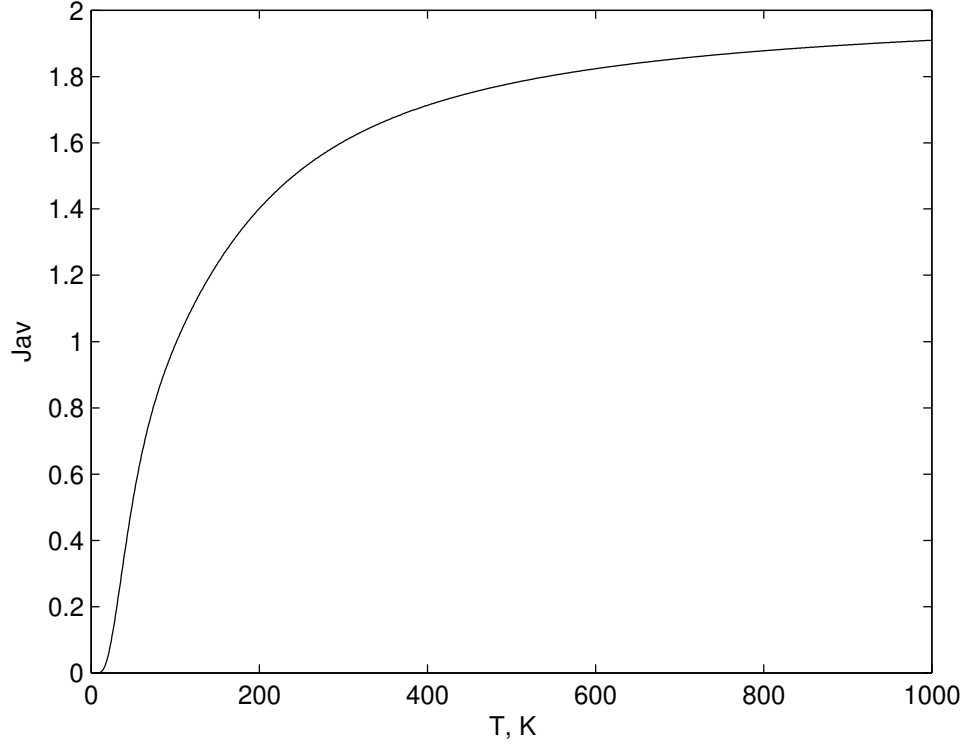


FIG. 4: The temperature dependence of the average local moment shows the spin-state transition from the nonmagnetic low spin state at $T = 0K$ to the paramagnetic high spin state at finite temperature. Only at $T \approx 1000K$ the moment is close to 2. In the region of the spin-state transition at $T \sim 100K$ $J_{av} \approx 1$.